Electronic Supplementary Material (ESI) for Journal of Materials Chemistry C.

Supporting information

Identification of distinctive structural and optoelectronic properties of Bi_2O_3 polymorphs controlled by tantalum addition

Taro Saito,[a]† Rafia Ahmad,[b]† Fuminao Kishimoto,[a] Tomohiro Higashi,[c] Masao Katayama,[d] Luigi Cavallo,*[b] Kazuhiro Takanabe*[a]

a. Department of Chemical System Engineering, School of Engineering, The University of Tokyo, 7-3-1, Hongo, Bunkyo-ku, Tokyo 113-8656, Japan

b. King Abdullah University of Science and Technology (KAUST), KAUST Catalysis Center (KCC), 4700 KAUST, Thuwal 23955-6900, Saudi Arabia

c. Institute for Tenure Track Promotion, University of Miyazaki, Nishi 1-1 Gakuen-Kibanadai, Miyazaki 889-2192, Japan

d. Environmental Science Center, Department of Chemical System Engineering, The University of Tokyo, 7-3-1, Hongo, Bunkyo-ku, Tokyo 113-8656, Japan

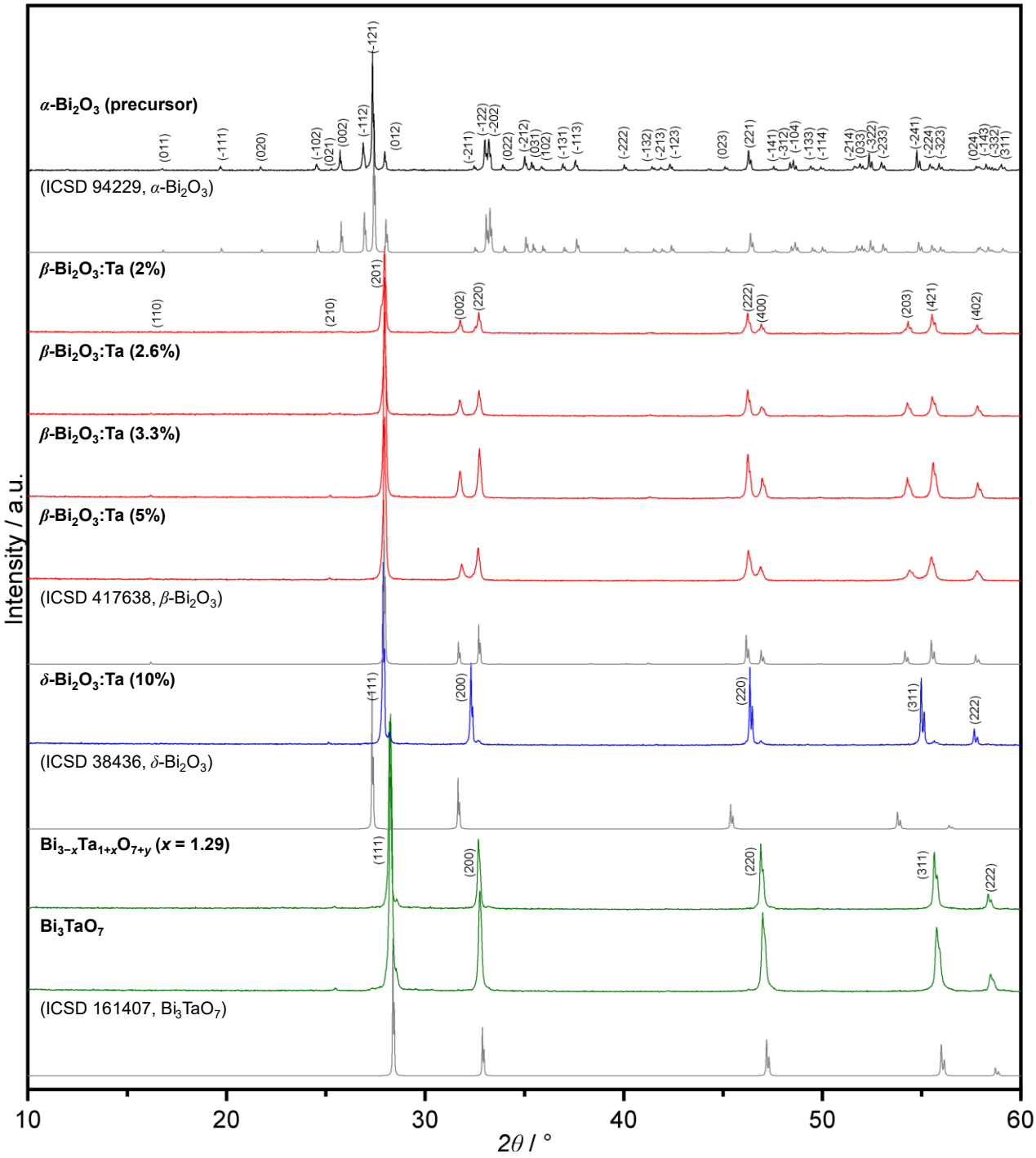

Figure S1. Detailed identifications of the XRD patterns and their reference patterns.

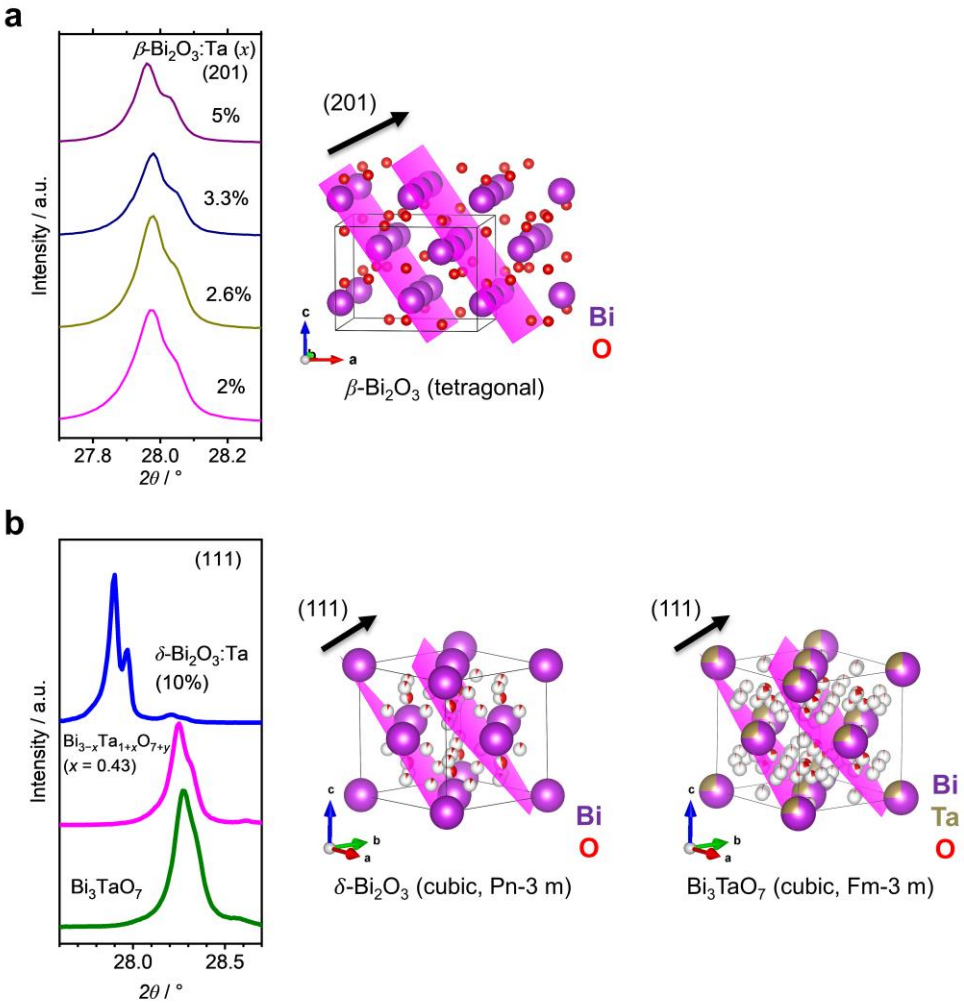

Figure S2. (a) The main peaks of the β-Bi_2O_3:Ta (2%), β-Bi_2O_3:Ta (2.6%), β-Bi_2O_3:Ta (3.3%), and β-Bi_2O_3:Ta (5%). (b) The main peaks of the δ-Bi_2O_3:Ta (10%), $Bi_{3+x}Ta_{1-x}O_{7-y}$ (x = 0.43) and Bi_3TaO_7.

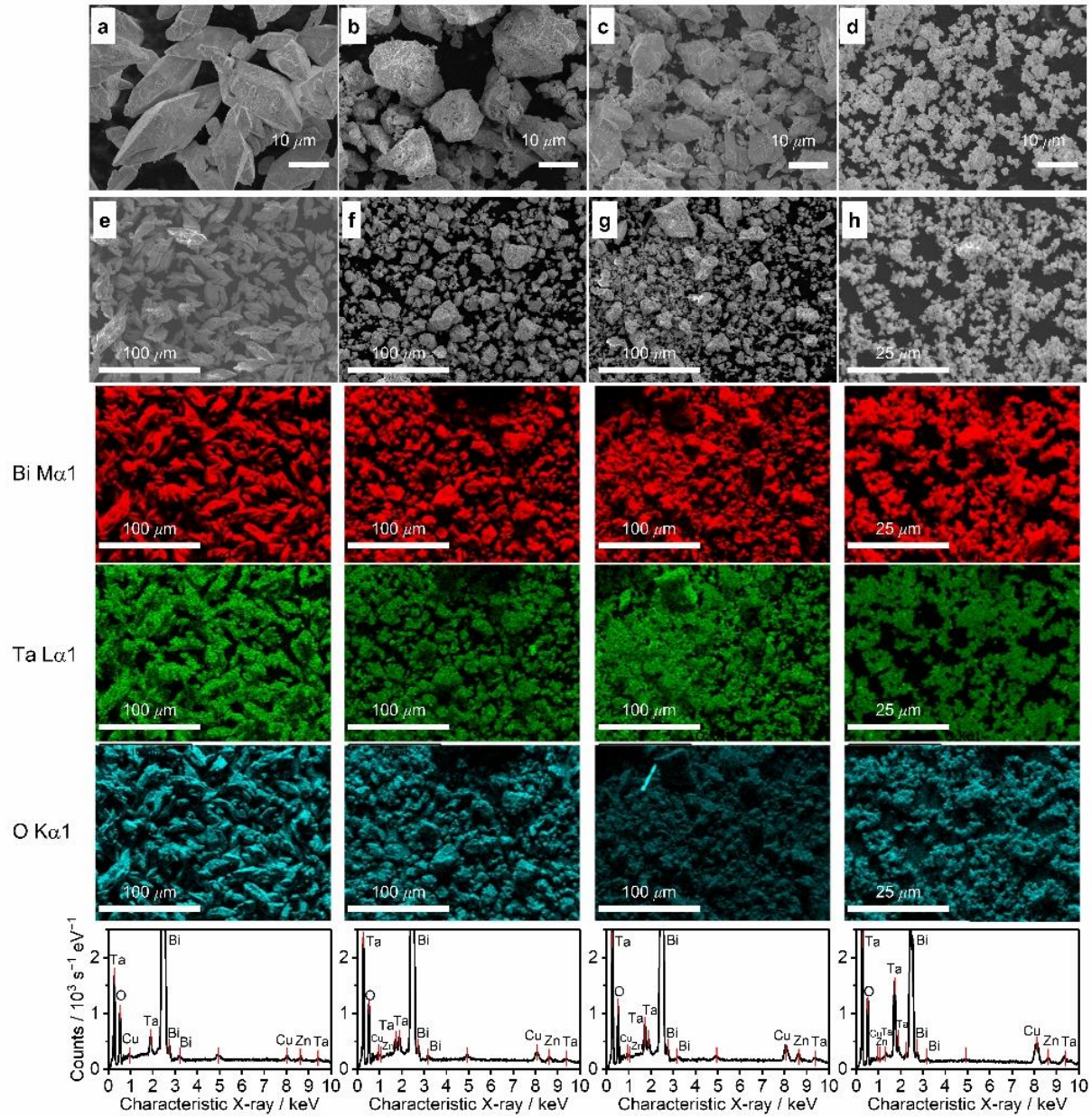

Figure S3. SEM images, EDS analysis and mappings of the (a)(e) α-Bi_2O_3 (precursor), (b)(f) β-Bi_2O_3:Ta (5%), (c)(g) δ-Bi_2O_3:Ta (10%), (d)(h) Bi_3TaO_7,

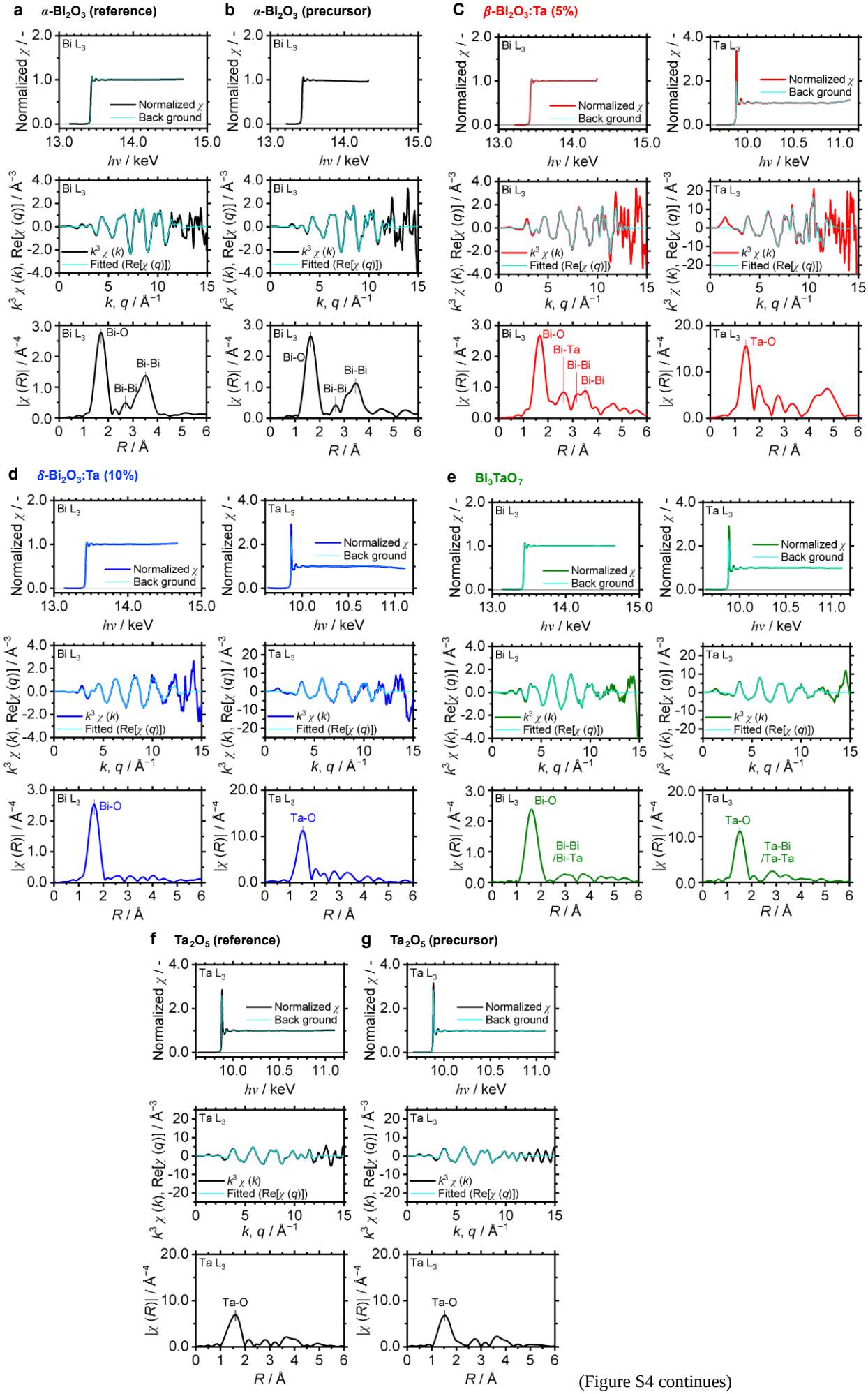

(Figure S4 continues)

h

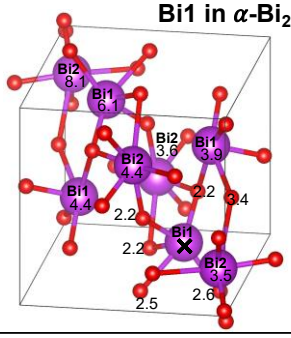

Bi1 in α-Bi_2O_3

	Distance / Å
Bi1-O	2.2, 2.2, 2.2, 2.5, 2.6, 3.4
Bi1-Bi2	3.5, 3.6
Bi1-Bi1	3.9, 4.4, 6.1
Bi1-Bi2	4.4, 8.1

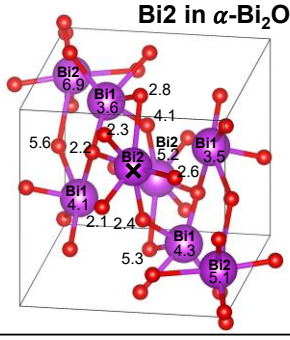

Bi2 in α-Bi_2O_3

	Distance / Å
Bi2-O	2.1, 2.2, 2.3, 2.4, 2.6, 2.8
Bi2-Bi1	3.5, 3.6
Bi2-O	4.1, 5.3, 5.6
Bi2-Bi1	4.1, 4.3
Bi2-Bi2	5.1, 5.2, 6.9

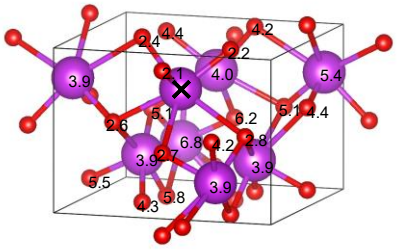

β-Bi_2O_3

	Distance / Å
Bi-O	2.1, 2.2, 2.4, 2.6, 2.7, 2.8
Bi-Bi	3.9, 3.9, 3.9, 3.9, 4.0
Bi-O	4.2, 4.4, 4.4, 5.1, 5.2, 5.5, 5.8, 6.2
Bi-Bi	5.4
Bi-Bi	6.8

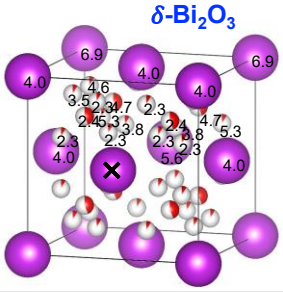

δ-Bi_2O_3

	Distance / Å
Bi-O	2.3, 2.4, 3.5, 3.8, 4.6, 4.7, 5.3
Bi-Bi	4.0, 5.6, 6.9

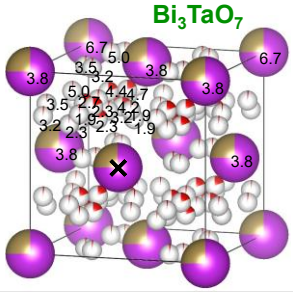

Bi_3TaO_7

	Distance / Å
M-O	1.9, 2.3, 2.7, 3.2, 3.5, 4.4, 4.7, 5.0
M-M	3.8, 6.7

M: Bi (75%) or Ta (25%)

Figure S4. Bi L_3 edge EXAFS in energy, *k* and *R* spaces of (a) α-Bi_2O_3 (reference) and (b) α-Bi_2O_3 (precursor). (c) Bi L_3 and Ta L_3 edge EXAFS in energy, *k*, and *R* spaces of the β-Bi_2O_3:Ta (5%). (d) Bi L_3 and Ta L_3 edge EXAFS in energy, *k*, and *R* spaces of the δ-Bi_2O_3:Ta (10%). (e) Bi L_3 and Ta L_3 edge EXAFS in energy, *k*, and *R* spaces of the Bi_3TaO_7. Ta L_3 edge EXAFS in energy, *k*, and *R* spaces of (f) Ta_2O_5 (reference) and (g) Ta_2O_5 (precursor). (h) Distances between a Bi atom and its neighboring atoms in the unit cells of α-Bi_2O_3 (ICSD 94229), β-Bi_2O_3 (ICSD 417638), δ-Bi_2O_3 (ICSD 38436) and Bi_3TaO_7 (ICSD 161407).

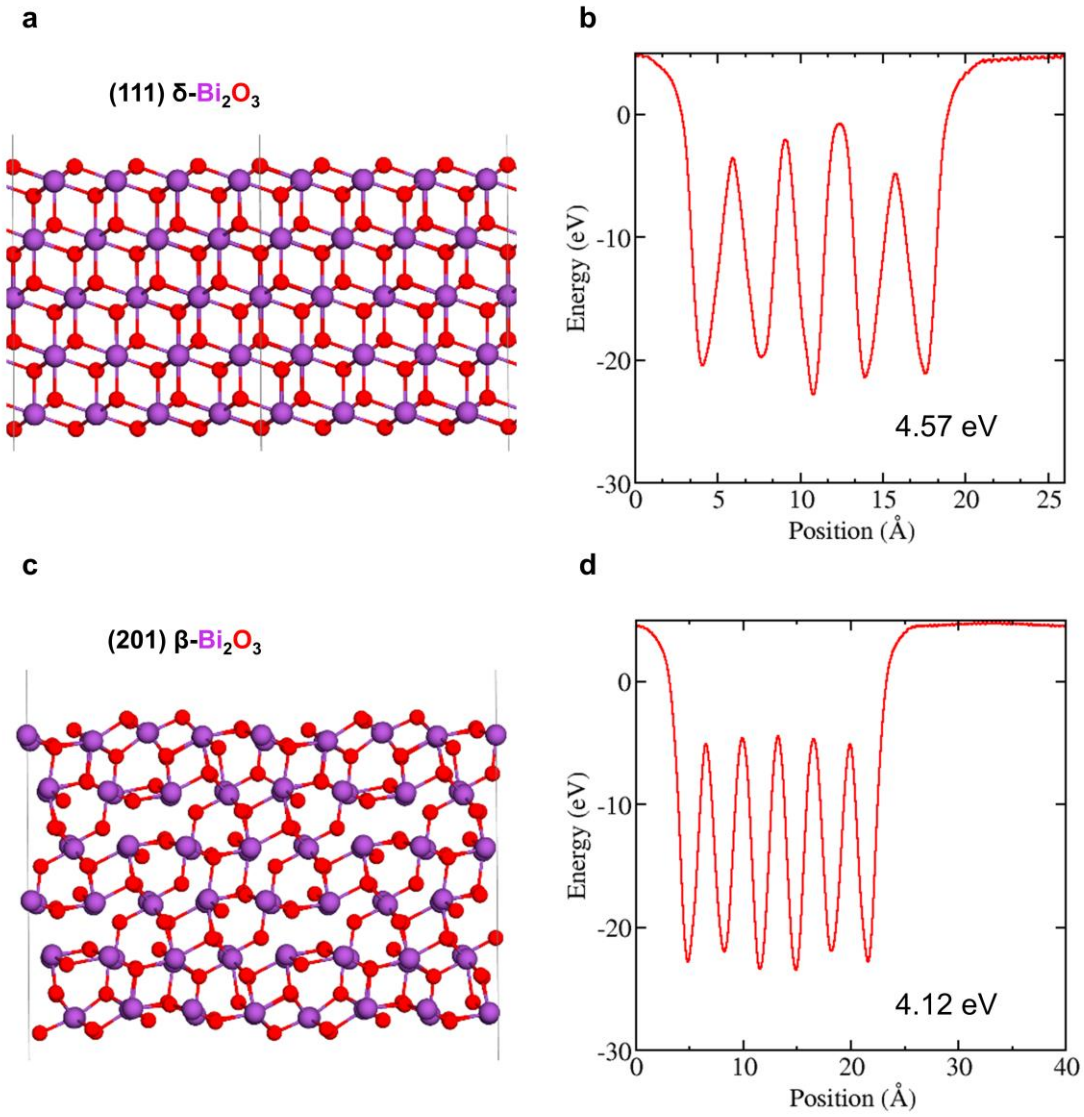

Figure S5 (a) The completely optimized structure, (b) the local potential with respect to the vacuum level in the z-direction, of a (111) slab of **δ-Bi_2O_3.** (c) The completely optimized structure, (d) the local potential with respect to the vacuum level in the z-direction, of a (201) slab of **β-Bi_2O_3.** The geometry optimization and electronic structure calculations were performed employing the HSE (Heyd–Scuseria Ernzerhof) exchange-correlation functional along with spin-orbit coupling corrections as implemented in VASP.

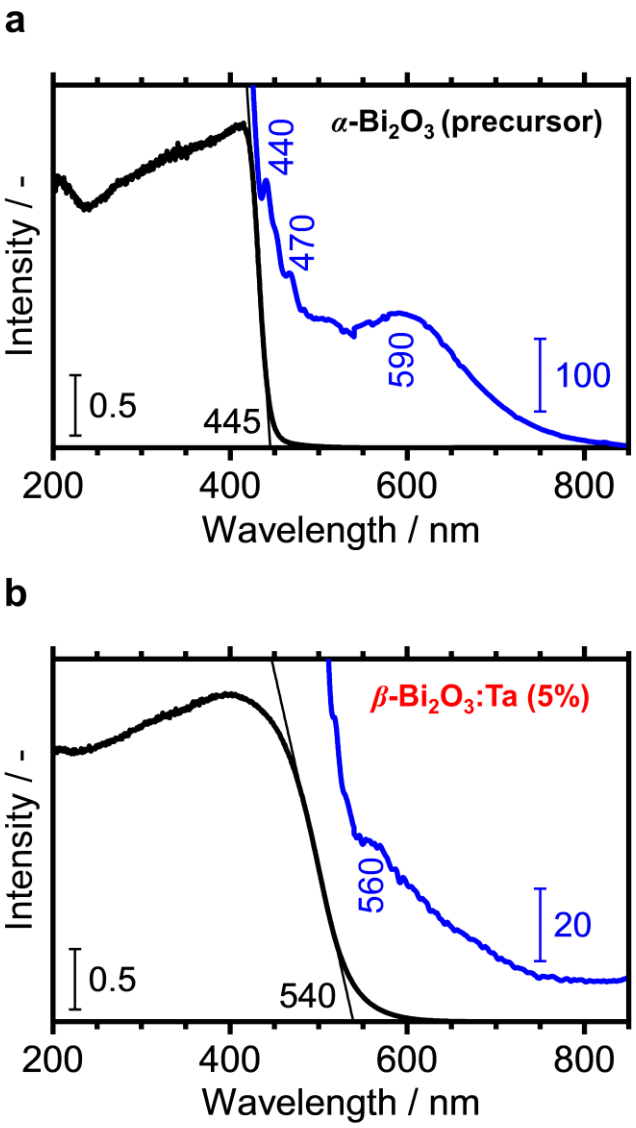

Figure S6 (a) Kubelka-Munk function (black) and PL spectrum (blue) of α-Bi_2O_3 (precursor). The emission spectrum under 400 nm was taken under 400 nm excitation light. (b) Kubelka-Munk function (black) and PL spectrum (blue) of β-Bi_2O_3:Ta (5%). The emission spectrum under 480 nm was taken under 480 nm excitation light.

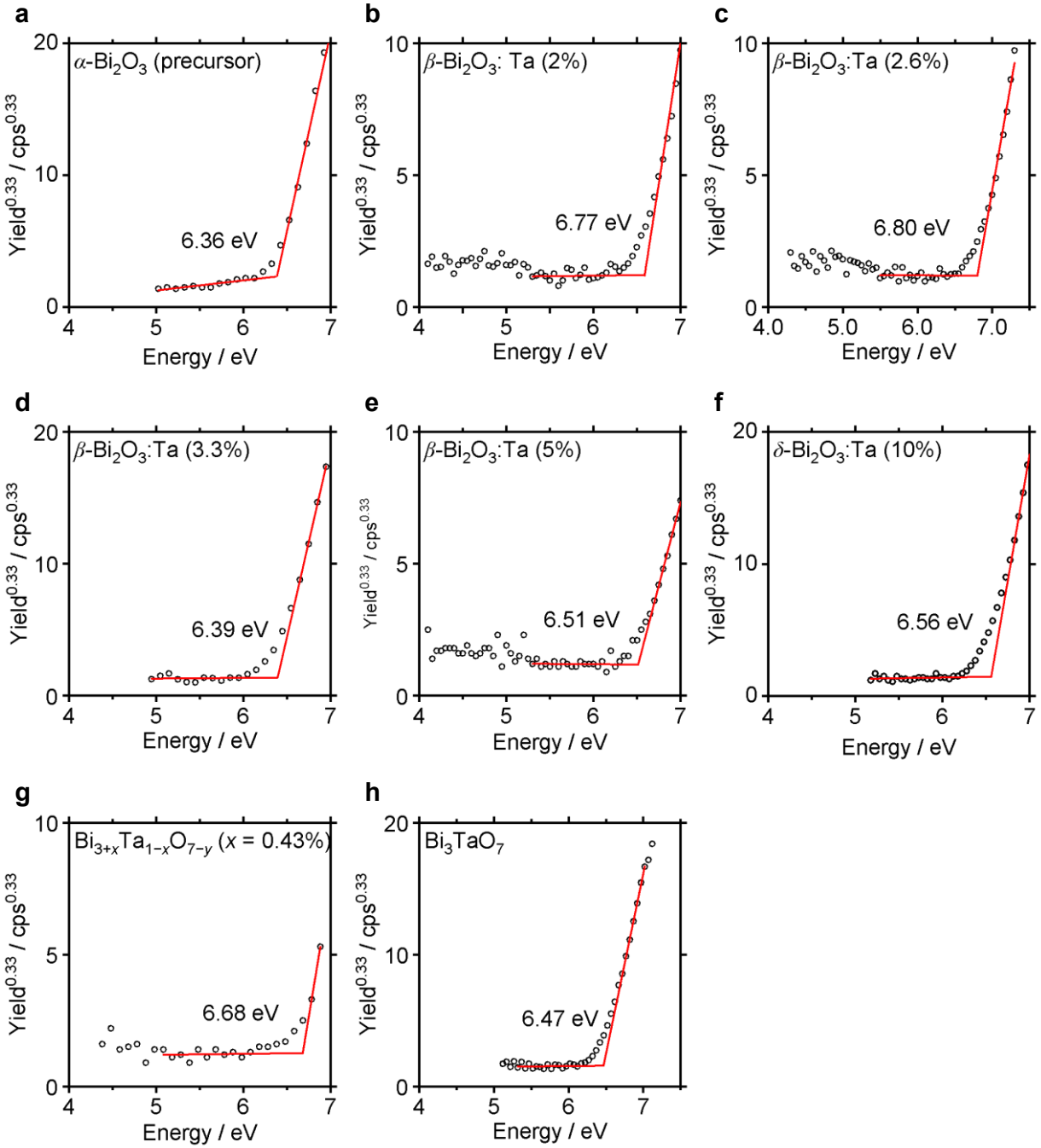

Figure S7. PESA. The spectra were calibrated based on the work function of Au (5.30 eV vs. vacuum).

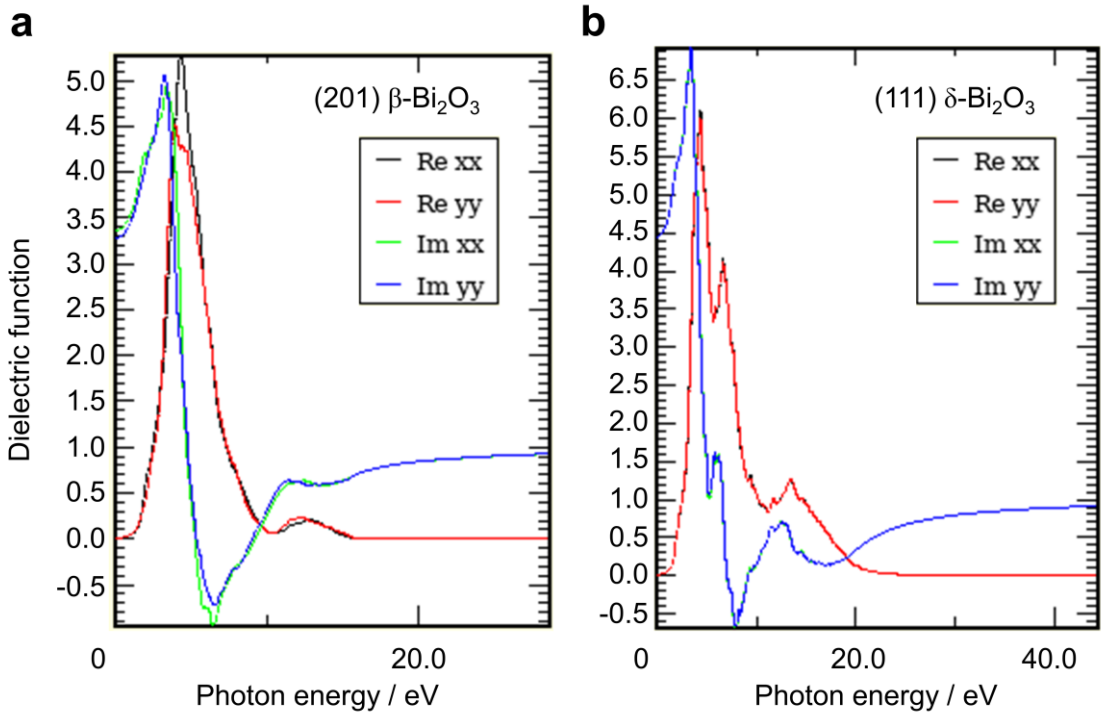

Figure S8. Real and imaginary parts of the dielectric function of (a) (201) β-Bi_2O_3 and (b) (111) δ-Bi_2O_3 obtained by HSE06 and SOC (spin-orbit coupling).

Theory of calculating dielectric constant and effective mass in VASP.

The surface simulations were performed by using the slab model, in which a finite number of crystal layers in a three-dimensional periodic-boundary-condition (PBC) cell is used to generate the experimentally observed surfaces through the introduction of a vacuum gap perpendicular to the surface. We modeled (201) and (111) facets of β-Bi_2O_3 and δ-Bi_2O_3, respectively following the evidence from the experiments. We keep a vacuum gap of 15 Å in the slab models with atleast 5 atomic layers, respectively. Monkhorst−Pack generated 9 × 9 × 1 k-point grids were used for the surface relaxation and the computations of density of states (DOS). Geometry optimizations were terminated when the energy and force on each ion were reduced below 10^{-6} eV and 0.02 eV/Å, and the optimized structures were then used to calculate the electronic structures.

To evaluate the light absorption capacity, the absorption coefficient can be calculated by the following formula:

$$\alpha(\omega) = \frac{\left(\sqrt{2}\,\omega\right)\left((\varepsilon_1^2 + \varepsilon_2^2 - \varepsilon_1)^{\frac{1}{2}}\right)}{2}$$

Where ε_1 and ε_2 are the real and imaginary parts of the dielectric function, and ω is the photon frequency. The optical properties were obtained from the frequency dependent dielectric response theory including local field effects in the random-phase-approximation (RPA) [M.S. Hybertsen, S.G. Louie**,** Phys. Rev. B, 34 (1986), p. 5390]. The dielectric tensor was calculated using the hybrid functional HSE06 in VASP.

The effective mass tensor (*m**) was obtained by fitting the two band edges of the calculated band structure with a parabolic function and calculating the 2nd derivative of the fitted function. The effective mass is defined as:

$$\left(\frac{1}{m^*}\right)_{ij} = \frac{\frac{1}{\hbar^2}\partial^2 E_n(k)}{\partial k_i k_j}\ (i,j = x,y,z)$$

where *x*, *y*, *z* are the directions in reciprocal Cartesian space, and $E_n(k)$ is the dispersion relation for the *n*-th electronic band. The result obtained from the bottom of the conduction band is the electron effective mass (m_e*) and the result obtained from the top of the valence band is the hole effective mass (m_h*). This is extremely expensive calculation in the hybrid functional HSE06 in VASP so to get a qualitative flavor of the difference between transport carriers' masses of (201) surface of β-Bi_2O_3 and (111) surface of δ-Bi_2O_3 we perform these calculations in PBE-GGA as implemented in VASP.